30. J. C. Bailey, O. Larsen, T. I. Frolova, *Contrib. Mineral. Petrol.* **95**, 155 (1987).
31. A. Zindler and S. R. Hart, *Annu. Rev. Earth Planet. Sci.* **14**, 493 (1986).
32. A.B.K. extends appreciation to J. B. Rundle, F. J. Ryerson, and G. Zandt for support. Logistical and field support from I. Kushiro and K. Kaneko is gratefully acknowledged. Reviews by K. Mezger, C. R. Stern, and two anonymous reviewers improved the manuscript. This work was funded by the Institute of Geophysics and Planetary Physics under the auspices of Department of Energy contract W-7405-Eng-48 and the Australian Research Council. This is publication 56 of the GEMOC Key Centre for teaching and research.

29 January 1996; accepted 18 April 1996

Amorphization of Serpentine at High Pressure and High Temperature

Tetsuo Irifune,* Koji Kuroda, Nobumasa Funamori, Takeyuki Uchida, Takehiko Yagi, Toru Inoue, Nobuyoshi Miyajima

Pressure-induced amorphization of serpentine was observed at temperatures of 200° to 300°C and pressures of 14 to 27 gigapascals with a combination of a multianvil apparatus and synchrotron radiation. High-pressure phases then crystallized rapidly when the temperature was increased to 400°C. These results suggest that amorphization of serpentine is an unlikely mechanism for generating deep-focus earthquakes, as the temperatures of subducting slabs are significantly higher than those of the rapid crystallization regime.

The occurrence of deep-focus earthquakes at depths of 100 to 670 km in the mantle has been a puzzle because the brittle fracture should be prohibited under the pressure and temperature conditions corresponding to these depths. A number of mechanisms have been proposed for the deep-focus earthquakes (*1*, *2*), but each has certain weaknesses. One proposed mechanism is pressure-induced dehydration and amorphization of serpentine, a major hydrous phase in the subducting oceanic lithosphere (*3*). Acoustic emissions have been associated with either the dehydration or amorphization of serpentine at pressures of up to 25 GPa in a diamond anvil cell (*2*). However, the direct observations of pressure-induced amorphization of serpentine were made at room temperature only. It has thus remained unclear whether the acoustic emissions observed between 6 and 25 GPa at temperatures of up to about 600°C (*2*) were actually related to the amorphization of serpentine. We therefore examined the temperature and pressure conditions for the amorphization of serpentine using in situ synchrotron radiation x-ray diffraction measurements and a double-stage multianvil high-pressure apparatus.

We used natural antigorite with a composition of $(Mg_{0.95}, Fe_{0.05})_3Si_2O_5(OH)_4$ as the starting material. We also used a natural lizardite to study the effect of the crystallographic form on amorphization. The powdered sample was mixed with a Au powder for pressure measurements (*4*) and enclosed in a capsule made of cemented amorphous boron. Twin-sheet heaters of TiC were used, and the temperature was monitored with a $W_{97}Re_3$-$W_{26}Re_{74}$ thermocouple (*5*). In situ x-ray diffraction measurements at high pressures and high temperatures were performed at the National Laboratory for High Energy Physics (KEK) with a hybrid anvil system (*6*).

We carried out four runs at pressures up to 28 GPa and at temperatures up to 1500°C (Fig. 1). For the first run (ME-1), containing antigorite, the pressure was increased slowly to 27 GPa at room temperature over 14 hours. The x-ray pattern was taken for 5 to 10 min after the pressure was held for 10 to 30 min every 2 to 3 GPa. Virtually no changes were observed in the diffraction patterns at pressures up to 27 GPa (Fig. 2, A and B); thus, no amorphization of antigorite was observed with compression at room temperature.

Next, the temperature of the sample was gradually increased to 1200°C over 6 hours at 27 GPa. Diffraction patterns were collected after every 50° to 100°C increase, and we monitored the pressure change at the fixed press load during the heating (*7*). The intensities of the diffraction peaks of antigorite decreased compared with those of Au at temperatures near 200°C, and the peaks disappeared at this temperature in a few minutes (Fig. 2C). A diffraction halo, characteristic of an amorphous material, appeared as the diffraction peaks disappeared; thus, antigorite was converted to an amorphous state at these temperatures within 10 min. With further heating, a few new diffraction peaks appeared at temperatures near 400°C, and these grew rapidly (Fig. 2, D and E). X-ray diffraction and electron microprobe data for the sample quenched from 1200°C at 24 GPa show the presence of phase D (*8*) and superhydrous B. Similar results were obtained with lizardite (run ME-3) at pressures of about 26 GPa (Fig. 1).

We also obtained similar results near 19 GPa (run ME-2, Fig. 3), except that amorphization of serpentine started at slightly higher temperatures (by ~ 50°C) (Fig. 1). The final products of this run, at 20 GPa and 1050°C, were γ-$(Mg, Fe)_2SiO_4$ + stishovite (+ water).

In contrast, at pressures of 10 to 13 GPa, we did not observe any clear evidence of amorphization of antigorite either at room temperature or at high temperatures (run ME-6, Fig. 1). Although the intensity of some diffraction peaks decreased slightly relative to those of Au at 400°C, high-pressure phases crystallized rapidly above 450°C. The quenched product from 1200°C at 11 GPa consisted of α-$(Mg, Fe)_2SiO_4$ + clinoenstatite (+ water).

Thus, in all of our runs, serpentine did not become amorphous over 14 to 30 hours

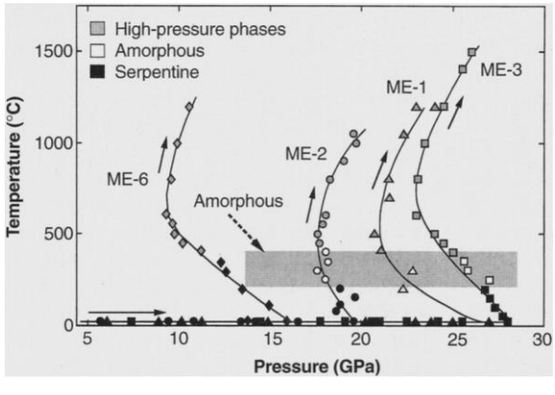

Fig. 1. The temperature and pressure conditions of in situ x-ray diffraction measurements and summary of the experimental runs to examine the amorphization of serpentine. Antigorite (ME-1, ME-2, and ME-6) and lizardite (ME-3) were used as starting materials. The "amorphous" region denotes the conditions where amorphization of serpentine was observed while no high-pressure phases were encountered.

T. Irifune and K. Kuroda, Department of Earth Sciences, Ehime University, Matsuyama 790, Japan.
N. Funamori, T. Uchida, T. Yagi, Institute for Solid State Physics, University of Tokyo, Roppongi, Minato-ku 106, Japan.
T. Inoue, Center for High Pressure Research, State University of New York, Stony Brook, NY 11794, USA.
N. Miyajima, Department of Earth and Planetary Sciences, Hokkaido University, Sapporo 060, Japan.
*To whom correspondence should be addressed.

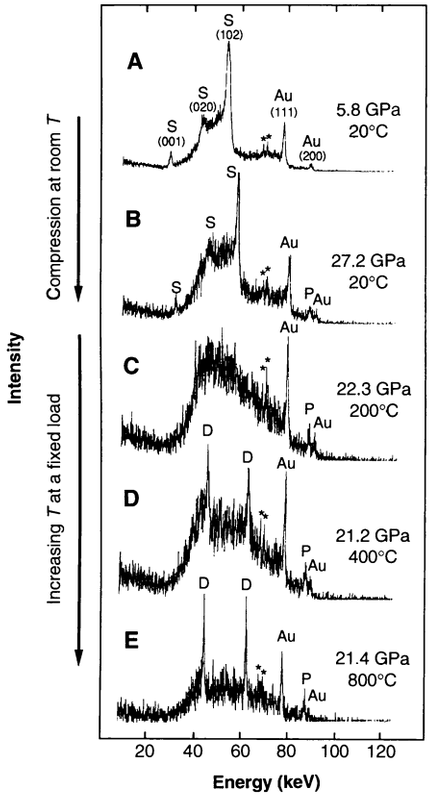

Fig. 2. Some examples of the x-ray diffraction patterns in run ME-1 taken at $2\theta = 4°C$, where θ is diffraction angle. Virtually no changes in the patterns were observed in antigorite upon compression to 27 GPa at room temperature (**A** and **B**), but it became amorphous above the temperature (T) of 200°C (**C**) at a fixed press load of 300 tons. At temperatures near and above 400°C, rapid crystal growth of phase D (peaks marked "D") was observed (**D** and **E**). Note that the halos observed in the energy interval of 40 to 80 keV are mostly caused by the amorphous boron capsule. Likewise, the peak identified as that of periclase is due to the magnesia pressure medium that surrounded the boron capsule. The additional halo became obvious in (C) and (D), where most of the antigorite became amorphous. S, serpentine (antigorite); Au, gold used as a pressure marker; P, periclase. Asterisks denote the characteristic x-ray lines of gold.

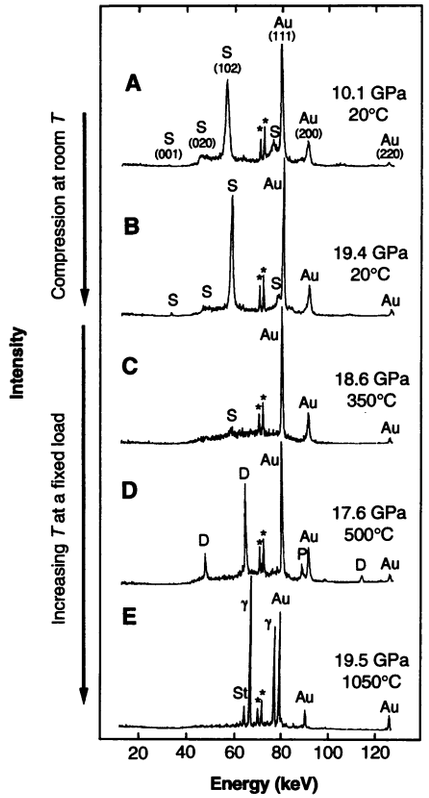

Fig. 3. (**A** through **E**) X-ray diffraction patterns at $2\theta = 4°C$ observed in run ME-2. Essentially the same results were obtained for the amorphization and the crystallization of antigorite as in the other runs, except that the final product observed at 19.5 GPa at 1050°C was the spinel form of $(Mg,Fe)_2SiO_4$ (γ) plus stishovite (St).

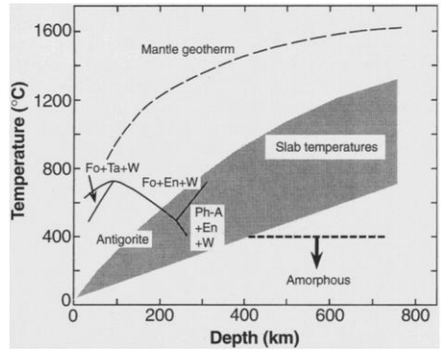

Fig. 4. Possible temperatures at the upper ~10 km of the subducting slabs as a function of depth (*2*, *12*). The temperatures of relatively young and thin slabs are higher than those of older and thicker ones, but most of these estimations fall in the shadow region. A typical mantle geotherm (*14*) is also shown for comparison. The present results suggest that the amorphization of serpentine should occur only at temperatures less than 400°C, which are well below the temperatures of the slabs. The phase relations of antigorite at depths shallower than 250 km are based on the results of a recent phase equilibrium study to 8 GPa (*11*). En, enstatite; Fo, forsterite; Ph-A, phase A; Ta, talc; W, water.

at pressures up to 28 GPa and at room temperature. These results are in contrast with those obtained with a diamond anvil cell, where gradual amorphization of serpentine was observed in a pressure interval between 6 and 22 GPa. This difference may be due to kinetic effects on the amorphization, as the diamond cell experiments were conducted over a longer time interval (*2*).

Alternatively, the difference between the results with the multianvil apparatus and the diamond anvil cell may be due to the different stress environments of the samples. The differential stress in a diamond cell is generally larger than that in a multianvil apparatus by about one order of magnitude (*9*, *10*). Although the mechanism of the pressure-induced amorphization is not fully understood, it is likely that such a transformation is enhanced by high differential stress by analogy with the effects of shear stress on pressure-induced phase transformations in olivine (*9*).

The results of a recent phase equilibria study (*11*) and the present experimental results on serpentine are summarized in Fig. 4. Pure antigorite dehydrates at 2 to 7 GPa and 600° to 700°C. Other forms of serpentine may dehydrate at significantly lower temperatures, and, accordingly, the dehydration mechanism seems appropriate for the cause of the acoustic emissions observed in lizardite at pressures up to 9 GPa at 600°C in the diamond anvil cell experiments. Some subducting slabs may be warmer than 600°C as indicated in Fig. 4, and the dehydration mechanism can probably cause the deep-focus earthquakes at depths above 200 to 300 km.

Our results show that amorphization of serpentine does occur between 14 and 26 GPa at temperatures less than 200° to 300°C (Figs. 1 and 4). However, at about 400°C, high-pressure phases rapidly crystallized in all of our runs. If longer run durations were available, crystallization might happen at lower temperatures. Thus, in subducting slabs, serpentine should completely transform to high-pressure phases at temperatures of 400°C, or probably lower. Although temperatures in subducting slabs are not well defined and vary among slabs, temperatures at about 10 km from the upper surface of the slab, where serpentine may be one of the major minerals, have been estimated to be 600° to 1200°C at a depth of 600 km (*12*); therefore, it seems unlikely that serpentine experiences the pressure-induced amorphization if it subducts to these depths (Fig. 4). It follows that the deep-focus earthquakes observed in a depth interval of 450 to 650 km are unrelated to the amorphization of serpentine. The preservation down to 650 km (*13*) of the fault zones, which were formed by the dehydration of serpentine at shallower depths (*2*, *11*), may be the major cause for the deep-focus earthquakes at these depths.

REFERENCES AND NOTES

1. H. Jeffreys, *Proc. R. Soc. Edinb.* **56**, 158 (1936); P. W. Bridgman, *Am. J. Sci.* **243A**, 90 (1945); D. T. Griggs, in *Nature of the Solid Earth*, E. C. Robertson, Ed. (McGraw-Hill, New York, 1972), pp. 361–384; C. M. Sung and R. G. Burns, *Tectonophysics* **31**, 1 (1976); M. Ogawa, *J. Geophys. Res.* **92**, 13801 (1987); S. H. Kirby, *ibid.*, p. 13789; H. W. Green II and P. C. Burnley, *Nature* **341**, 733 (1989); H. W. Green II, T. E. Young, D. Walker, C. H. Scholz, *ibid.* **348**, 720 (1990).
2. C. Meade and R. Jeanloz, *Science* **252**, 68 (1991).

3. M. Cannat *et al.*, *Geology* **23**, 49 (1995).
4. The pressures both at room temperature and at high temperatures were estimated on the basis of the unit cell volume changes of Au with an equation of state [O. L. Anderson, D. G. Isaak, S. Yamamoto, *J. Appl. Phys.* **65**, 1534 (1989)].
5. There were significant temperature gradients across the sample charge, and the uncertainty of the temperature measurements may be on the order of ±50°C, though we tried to examine the sample that was very close (~0.1 mm) to the hot junction of the thermocouple.
6. The hybrid anvil system [T. Irifune, W. Utsumi, T. Yagi, *Proc. Jpn. Acad.* **68**, 161 (1992)] uses four tungsten carbide (WC) and four advanced diamond composite (ADC) anvils for the double-stage anvil (MA8) system. The assembled anvil cube was pressurized in cubic presses (MAX80 and MAX90) at KEK [O. Shimomura, W. Utsumi, T. Taniguchi, T. Kikegawa, T. Nagashima, in *High-Pressure Research: Application to Earth and Planetary Sciences*, Y. Syono and M. H. Manghnani, Eds. [Terra Scientific (TERRAPUB)/American Geophysical Union (AGU), Tokyo/Washington, DC, 1992), pp. 3–11]. A white x-ray beam from the synchrotron radiation was introduced from the anvil gap through vertical (300 μm) and horizontal (50 μm) slits and irradiated onto the sample near the hot junction of the thermocouple. The diffracted x-ray beam was collected through vertical (500 μm) and horizontal (50 μm) slits at the fixed positions of $2\theta = 4°$ and 6°. An energy dispersive method was adopted with a solid-state detector and a multichannel analyzer. One of the ADC anvils was used for the window to direct the diffracted x-ray beam, because this material is highly transparent to the x-ray of a wide range of photon energies.
7. While the temperature was increased to about 500°C, the pressure dropped significantly (Fig. 1), probably because the pyrophyllite gaskets yielded as a result of stress relaxation within the sample. At still higher temperatures, however, the pressure increased again and approached the initial value.
8. The x-ray diffraction peaks of the quenched sample, after subtracting a few peaks that correspond to superhydrous B, were consistent with those of phase D [L. Liu, *Phys. Earth Planet. Inter.* **49**, 142 (1987)]. The phases in the products from our runs, however, contained about 15 weight % H_2O as estimated from the deficit of the oxide total of the electron microprobe analysis and had a Si/Mg ratio of ~1.5, which is quite different from that proposed for phase D. This composition is rather close to that of phase F synthesized at pressures above 15 GPa [M. Kanzaki, *ibid.* **66**, 307 (1991)], but our x-ray diffraction pattern is completely different from those reported for phase F [Y. Kudoh, T. Nagase, S. Sasaki, M. Tanaka, M. Kanzaki, *Phys. Chem. Mineral.* **22**, 295 (1995)].
9. T. Wu, W. A. Bassett, P. C. Burnley, M. S. Weathers, *J. Geophys. Res.* **98**, 19767 (1993).
10. K. Fujino and T. Irifune, in *High-Pressure Research: Application to Earth and Planetary Sciences*, Y. Syono and M. H. Manghnani, Eds. (TERRAPUB/AGU, Tokyo/Washington, DC, 1992), pp. 237–243.
11. P. Ulmer and V. Trommsdorff, *Science* **268**, 858 (1995).
12. D. L. Turcotte and G. Schubert, *Geodynamics* (Wiley, New York, 1982); G. R. Helffrich, S. Stein, B. J. Wood, *J. Geophys. Res.* **94**, 753 (1989); S. H. Kirby *et al.*, *Science* **252**, 216 (1991).
13. P. G. Silver *et al.*, *Science* **268**, 69 (1995).
14. E. Ito and T. Katsura, *Geophys. Res. Lett.* **16**, 425 (1989).
15. We thank S. Urakawa, T. Ohtani, K. Fujino, T. Kikegawa, O. Shimomura, and M. Miyashita for their help and encouragement during the x-ray diffraction experiments at KEK. The antigorite specimen was provided by T. Minakawa. Supported by Grant-in-Aid for Scientific Research from the Ministry of Education, Science and Culture of the Japanese Government, and by the Japan Society for the Promotion of Science.

12 February 1996; accepted 18 April 1996

Blockage by Adenovirus E4orf6 of Transcriptional Activation by the p53 Tumor Suppressor

Thomas Dobner, Nobuo Horikoshi, Susanne Rubenwolf, Thomas Shenk*

The adenovirus E4orf6 protein is shown here to interact with the cellular tumor suppressor protein p53 and to block p53-mediated transcriptional activation. The adenovirus protein inhibited the ability of p53 to bind to human $TAF_{II}31$, a component of transcription factor IID (TFIID). Earlier work demonstrated that the interaction of p53 with $TAF_{II}31$ involves a sequence near the NH_2-terminus of p53, whereas the E4orf6-p53 interaction occurs within amino acids 318 to 360 of p53. Thus, the E4orf6 protein interacts at a site on p53 distinct from the domain that binds to $TAF_{II}31$ but nevertheless inhibits the p53-$TAF_{II}31$ interaction.

The transcriptional regulatory protein p53 (*1*) activates the expression of proteins that control cellular growth (*2*). Inhibition of its ability to activate transcription correlates with oncogenesis (*3*). Three functional domains of p53 have been defined (*4*): an NH_2-terminal transcriptional activation domain (amino acids 1 to 42), a central DNA binding domain (amino acids 120 to 290), and a COOH-terminal regulatory domain (amino acids 311 to 393). The DNA binding domain recognizes a DNA motif in genes that are activated by p53 (*5*). Mutations in p53 that arise in human cancers generally cluster in its DNA binding domain (*6*). The NH_2-terminal activation domain stimulates transcription by interacting with $TAF_{II}31$, a constituent of TFIID, in the transcriptional initiation complex (*7*). The MDM-2 oncoprotein (*8*) and the adenovirus E1B 55-kD oncoprotein (*9*) each bind to this domain of p53, blocking its activation function. The COOH-terminal domain of p53 contains an oligomerization domain as well as sequences that modulate DNA binding by p53. An antibody that binds within this domain stimulates sequence-specific DNA binding by p53 (*10*), as does phosphorylation within this domain (*10–13*). The COOH-terminal domain of p53 also can bind to single-stranded nucleic acids (*4*, *14*, *15*), and short single strands of DNA markedly stimulate sequence-specific DNA binding by the central domain of p53 (*15*). In this report, we demonstrate that the adenovirus E4orf6 protein binds to the COOH-terminal regulatory domain of p53. However, rather than modulate DNA binding, the viral protein inhibits the interaction of the NH_2-terminal activation domain with the transcriptional initiation complex.

The adenovirus E1B 55-kD protein can bind to both p53 (*9*) and the adenovirus E4orf6 protein (*16*), which raises the possibility that the three proteins might form a complex within adenovirus-infected cells. Therefore, we examined whether the E4orf6 protein can influence transcriptional activation by p53 (*17*). Initially, we assayed the effect of E4orf6 on the activity of a reporter gene containing two copies of the p53 binding site from the muscle creatine kinase gene in p53-deficient SAOS-2 cells (Fig. 1A). Cotransfection of a plasmid expressing p53 with the reporter enhanced expression by a factor of about 6, whereas inclusion of a third plasmid expressing the E4orf6 protein blocked the ability of p53 to enhance expression from the reporter. In control experiments (Fig. 1A), an E1B 55-kD protein expression plasmid blocked p53-mediated induction of the reporter as predicted (*9*); the expression cassette without an inserted E4orf6 complementary DNA (pDCR) had no effect on activation by p53, which rules out the possibility that the inhibition observed was the result of promoter competition.

The E4orf6 protein also blocked the induction of a reporter gene containing Gal4 DNA binding sites by a Gal4-p53 fusion protein within HeLa cells (Fig. 1B). The E4orf6 protein inhibited activation by Gal4-p53 in a dose-dependent fashion as efficiently as the E1B 55-kD protein did. The expression cassette without the E4orf6 insert (pDCR) did not influence expression from the reporter (Fig. 1B); expression of the Gal4 DNA binding domain with no fusion partner (pSG424) did not influence activity of the reporter (Fig. 1C). Although expression of

T. Dobner and S. Rubenwolf, Institut für Medizinische Mikrobiologie und Hygiene, Universität Regensburg, D-93042 Regensburg, Germany.
N. Horikoshi and T. Shenk, Howard Hughes Medical Institute, Department of Molecular Biology, Princeton University, Princeton, NJ 08544, USA.

*To whom correspondence should be addressed.